Easy Tuning of Surface and Optical Properties of PDMS Decorated by Ag Nanoparticles

Easy tuning of surface and optical properties of PDMS decorated by Ag nanoparticles

A. Lamberti,[a*] *A. Virga,*[a] *P. Rivolo,*[a] *A. Angelini,*[a] *F. Giorgis*[a]

[a] Department of Applied Science and Technology, Politecnico di Torino, C.so Duca degli Abruzzi 24 10129, Torino, ITALY

ABSTRACT

Herein we report a systematic study on the wetting and optical properties of PDMS surface coated by silver nanoparticles. Uniform Ag nanoparticles distribution onto PDMS membrane was obtained through d.c room-temperature sputtering. The effect of sputtering current and PDMS mixing ratio between oligomer and curing agent was investigated by means of UV-Vis spectroscopy and contact angle measurements. The results clearly show that the wettability and optical properties of the silver-coated elastomeric substrate were strongly affected by the sputtering current and by the PDMS composition with a marked decrease of the water contact angle and the spectral shift of well-defined plasmonic dips in the transmittance spectra related to the nanoparticles morphology. Finite Element Method was employed to model the optical experimental results. The observed tunable properties can find huge application in several technological fields in which PDMS was usually employed as structural and/or plasmonic active element.

INTRODUCTION

PolyDiMethylSiloxane (PDMS) is one of the most employed polymer in the micro- and nano-technology field.[1-4] Its enormous potential and ever increasing popularity mainly reside in its intrinsic smart properties: cost effective, ease of fabrication process, high dielectric coefficient, biocompatibility, optical transparency, flexibility/stretchability and oxygen permeability.[5-8] The various outstanding properties of PDMS are basically due to the presence of methyl groups along the Si-O-Si backbone which confers to the elastomer a low surface energy and high thermal stability along with chemical and biological inertness. Thanks to the above mentioned characteristics, in the last decades it has been employed for the fabrication of several kind of devices such as biosensors,[9,10] tactile sensors,[11,12] lab-on-a-chip,[13,14] energy harvesters[15,16] and actuators.[17,18]

In all the main fields of application of PDMS its surface properties have a crucial importance in determining the final performances. Previous works have demonstrated that varying the mixing ratio of the bi-component elastomer precursors it is possible to strongly influence the surface properties of cross-linked material.[19,20] Another way aimed to modify the PDMS surface features such as its wettability concerns with depositing or embedding different kind of nanostructures within the elastomeric surface.[21,22] However there are not reports about the combination of the last two approaches.

Moreover the PDMS optical properties are of fundamental importance for its microfluidic application where high transparency[23] or tunable absorption windows[24] are required.

Herein, we reported on the d.c. sputtering deposition of Ag nanoparticles (NPs) onto PDMS membranes with different mixing ratio of the pre-polymer and curing agent. The obtained Ag-coated substrates were deeply characterized by contact angle analysis, electron microscopy and optical measurements (FTIR and UV-Vis transmittance spectroscopies), demonstrating the easy tuning of wettability and absorption/scattering windows of the prepared material.

EXPERIMENTAL SECTION

Ag-coated PDMS membranes fabrication.

PDMS pre-polymer and curing agent (Sylgard 184, Dow Corning) were mixed with different weight ratios (3:1, 5:1, 10:1, 20:1) and degassed at room temperature for 1 h. The mixtures were then casted into milling machined PMMA mold and cured at 80°C for 1 hour in a convection oven. In this way PDMS membrane with thickness of 500 µm and areas of 6 cm^2 can be obtained.

Ag nanoparticles were deposited at room temperature by d.c. sputtering in Ar atmosphere 10^{-4} bar (Q150T-ES, Quorun Technologies) using sputtering currents in the range 20-40 mA for 5 seconds.

In order to allow a qualitatively morphology characterization of the PDMS surface at the different mixing ratio by optical microscopy, a 100 nm thick Pt film was deposited on selected samples by d.c. sputtering at room temperature in Ar atmosphere 10^{-4} bar (Q150T-ES, Quorun Technologies) using sputtering current of 50 mA for 180 seconds..

Characterization methods

Fourier transformed infrared (FTIR) spectra were recorded using a Nicolet 5700 FTIR Spectrometer with 4 cm^{-1} resolution and an average of 64 scans. FTIR was performed on PDMS substrates to examine the dependence of material composition on different mixing ratios.

FESEM micrographs of sputtered samples were obtained as secondary electron images with 5 keV electrons using a Zeiss Supra 40 Field Emission Scanning Electron Microscopy.

Optical transmittance of the Ag-coated PDMS membrane was measured by a *PerkinElmer LAMBDA* 35 spectrophotometer in the wavelength range 300-700 nm. Five sample were prepared for each set of conditions exhibiting identical optical response.

The wetting behaviour of the samples was evaluated by contact angle measurements by the sessile drop technique with an OCA H200 instrument (DataPhysic Instruments GmbH) in ambient conditions. A DI-water drop with a volume of 1.5 μL was dispensed, and the image of the drop on the sample was acquired with the integrated camera. The drop profile was extracted and fitted through the Young–Laplace method, and contact angles between fitted function and base line were calculated by the SCA20 software that returned the contact angle value at the liquid–solid interface. For each sample, four drops were dispensed at different positions on the surface and the average value was calculated.

Strip tests were performed on the sample surface to evaluate the Ag nanoparticles adhesion with a commercial scotch tape. In particular, the eventual mass removal was studied for selected samples by comparing the UV-Vis transmittance spectra taken before and after the test.

A ZEISS optical microscope (Scope A1-Axio) was used to qualitatively characterize the Pt coated PDMS surface at the different mixing ratio.

RESULTS AND DISCUSSION

The cross-linking of PDMS into an elastomer is obtained via hydrosilylation in which vinyl groups of one component (prepolymer) react with hydrosilane groups of the other component (curing agent) in a platinum catalysed reaction.

The dependence of cross-linked PDMS membranes by the curing agent concentration was studied by FTIR analysis. In Figure 1 the spectra recorded by PDMS samples fabricated varying the mixing ratio from 3:1 up to 20:1 are reported. In the zoom it is possible to appreciate the intensity reduction of the bands associated to the cross-linker (bending Si–H at 910 cm^{-1}) and the opposite behaviour for the bands characteristic of the oligomers (stretching Si–O–Si at 1010 and 1054 cm^{-1}).

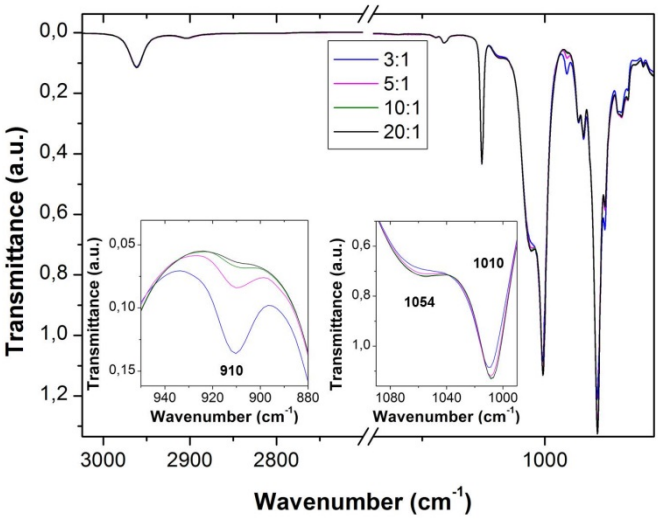

Figure 1. *FTIR transmittance spectra for PDMS at different mixing ratio (oligomer:crosslinker): 3:1, 5:1, 10:1, 20:1. In the inset the zooms make evident the fundamental changes.*

Just after Ag deposition it was possible to appreciate a strong colour variation depending on sputtering current and PDMS composition (see insets Figure 2). The colour of the noble-metal coated substrates is strictly dependent on the plasmonic response. [Hulteen, J. C., Patrissi, C. J., Miner, D. L., Crosthwait, E. R., Oberhauser, E. B., & Martin, C. R. (1997). Changes in the shape and optical properties of gold nanoparticles contained within alumina membranes due to low-temperature annealing. *The Journal of Physical Chemistry B*, *101*(39), 7727-7731.] In particular, all the transmittance spectra obtained on the metal-elastomeric nanostructures are characterized by dips corresponding to plasmon resonances ascribed to enhanced absorption/scattering processes related to Localized Surface Plasmons (LSP) coupled either to individual particles or through inter-particle interactions.

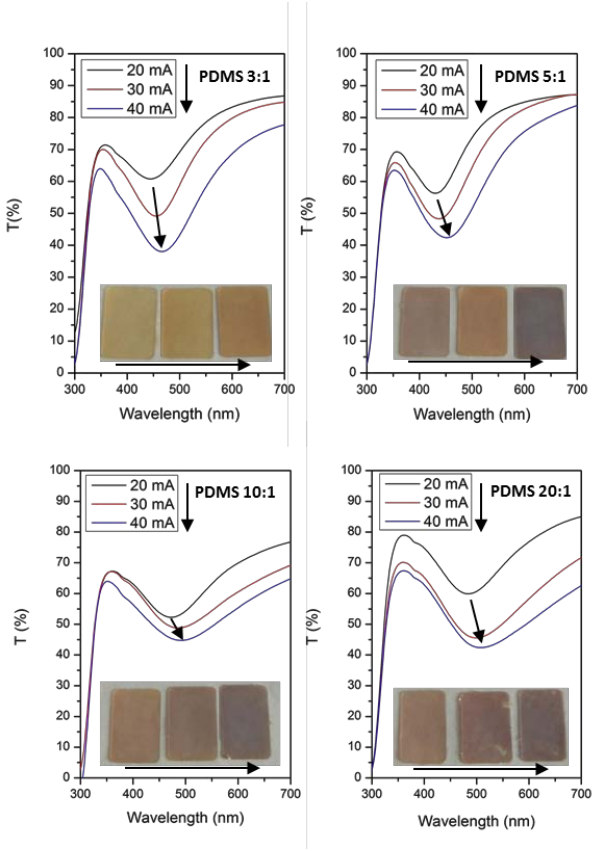

Figure 2. *Transmittance spectra of PDMS membrane coated with Ag nanoparticles by sputtering deposition varying the PDMS mixing ratio and the sputtering current at a fixed deposition time of 5 seconds. In the insets digital photographs of the Ag coated PDMS for all the composition and sputtering current are shown. The black arrows indicate the trend of the plasmon resonance spectral shift increasing the deposition current.*

On the other hand, theoretical and experimental analysis performed on elastomeric membranes decorated by Ag/Au nanoparticles yielded the dominance of inter-particle effects.[25-27] Actually, taking into account LSP coupled to particle dimers, a shift of the plasmon resonances can be observed by changing the particle density and the average particle size. Indeed, the main plasmon resonance is subjected to a spectral blue-shift by increasing the inter-particle nanogap[27], while fixing the gap, the increase of the particle size induces a red-shift. Such behaviour can be easily verified by analysing the near-field EM intensity spectra within Ag dimer nanogaps. To this aim, the optical response of Ag dimer of several

size and inter-particle gap deposited on a PDMS membrane has been modelled by 3D Finite Element Method (COMSOL Multiphysics software). The nanoparticles were modelled with a hemispherical shape, consistently with the model of noble metal clusters previously derived by Santoro and coworkers [Santoro et al., Appl. Phys. Lett., 2012, 104, 243107] discussed in terms of grazing incidence X-Ray scattering (GIXS) characterization and corroborated by TEM analysis reported by Han et al. [Han et al., J. Phys. Chem. Lett. 2014, 5, 131]. Moreover with the aim of obtaining a clear nanostructural proof of the particle shape we have performed cross-sectional FESEM characterization of silver nanoparticles (see Figure S1 in the Supporting Information).

As clearly shown in Figure 3, the EM intensity spectra (incident electric field polarized along the dimer axis) are characterized by a strong resonance which is subjected to a blue-shift and to an intensity quenching by increasing the inter-particle gap. This is observed for several fixed hemisphere diameters (see Figure 3b).

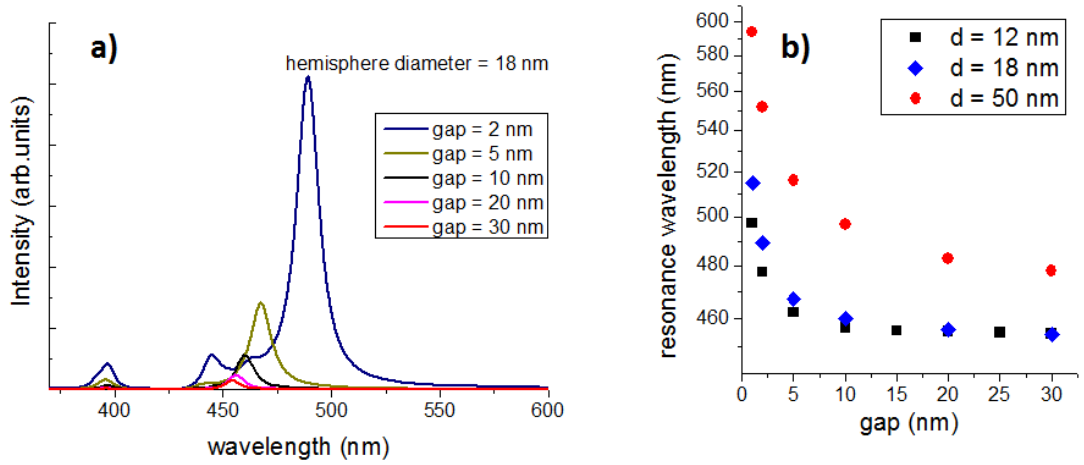

Figure 3. *(a) Calculated EM near-field intensity spectra within the nanogap of a dimer consisting in Ag hemispheres loaded on PDMS (sphere diameter = 18 nm). The spectra are related to different inter-particle gap (d = 2–30 nm). Incident electric field polarized along the dimer axis. (b) Spectral position of the main resonance for dimers characterized by several diameters and inter-particle gaps.*

In our samples, the increase of the sputtering current gives a red-shift of the plasmonic dip for all the PDMS substrates synthesized with different mixing ratio. Thus, a Ag nanostructured network with an increase of both the particle size and the particles density (i.e. shrinking on the inter-particle gap) can be foreseen. Figure 4a shows the calculated EM intensity spectra within the gap of two specific Ag dimers (depicted in Figure 4b,c). For dimers with increased size and decreased gap a spectral red-shift is evidenced. It is worth to underline that beside the NPs morphology, the effect of the dielectric substrate must be taken into account both for the LSP resonance energies and for the fields spatial localization.[28,29] However, the influence of the different pre-polymer and curing agent mixing ratios used for the synthesis of the PDMS membranes on their refractive index variation can be considered negligible, giving instead an effective influence on the nucleation of Ag NPs successively grown by d.c. sputtering.

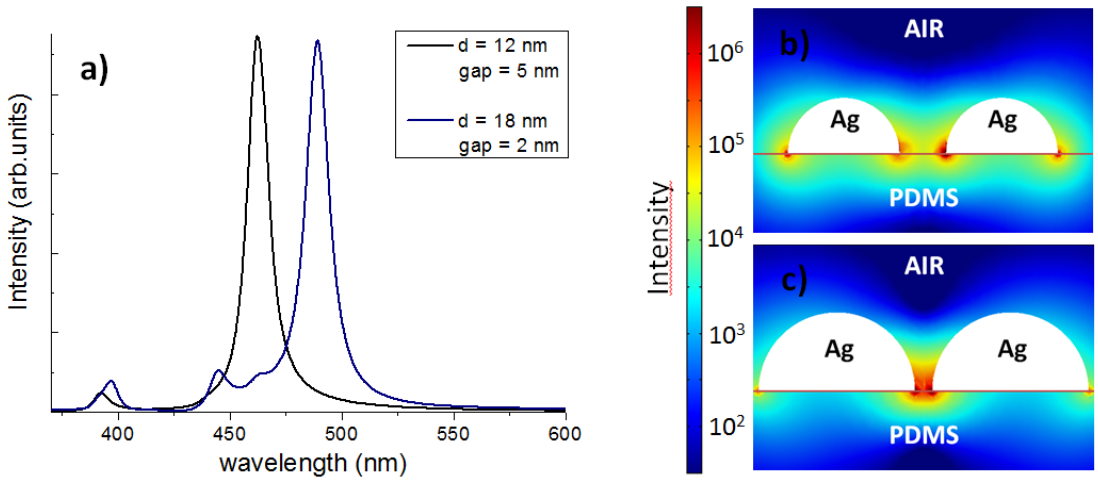

Figure 4. *(a) Calculated EM near-field intensity spectra (normalized to the intensity maximum) within the nanogap of a couple of dimers (sphere diameter = 12 nm and gap = 5 nm and sphere diameter = 18 nm and gap = 2 nm respectively).(b,c) Near-field intensity distribution at the resonance wavelength for the two dimers.*

Scanning electron microscope was used to investigate the effect of the sputtering current on silver NPs size and surface density. FESEM micrographs on the samples subjected to the

lowest (20 mA) and the highest (40 mA) sputtering current are reported in Figure 5 a) and b) respectively.

The FESEM images were analyzed using a homemade MATLAB routine to obtain the distribution of nanoparticles size and gaps between neighboring nanoparticles.[30] The increase of sputtering current leads to an increment in the number of ionized argon atoms, increasing the in-flight sputtered silver atom density in the deposition flux. The effect of this phenomenon is shown in Figures 5a,b where the results of images analysis are reported: at low current (20 mA), the nanoparticles are nucleating and growing starting a coalescence process between neighboring small particles which yields a bimodal distribution size; at higher current (40 mA), the nanoparticles increase their average size and size distribution, in particular, the coalescence process reduce their density and the average gap between them.[31] This is in agreement with the spectral shift of the plasmon dips experimentally found in samples synthesized with different sputtering current, taking into account the results yielded by the modelled Ag dimers previously discussed.

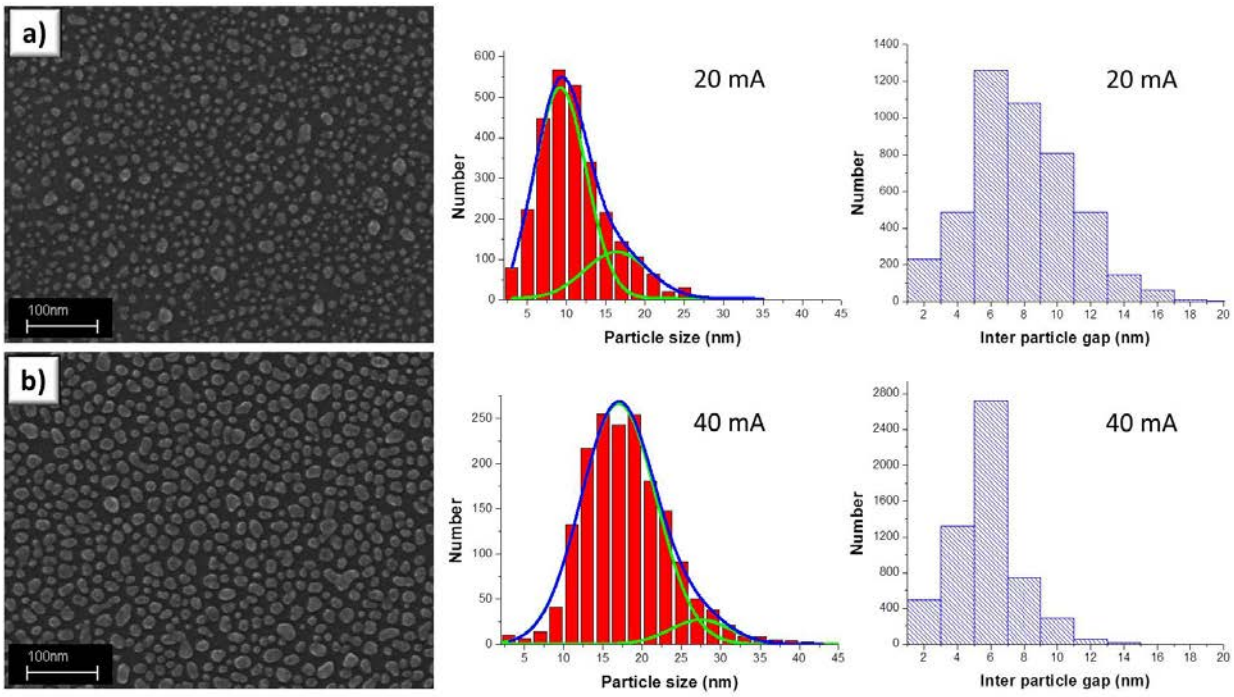

Figure 5. *FESEM micrographs Ag nanoparticles obtained by sputtering at 20 mA (a) and 40 mA (b). Distributions of nanoparticles size and gaps between neighbouring nanoparticles are also shown. The size distributions* were fitted with 2 Gaussian curve emphasizing the partial bimodal distribution at 20mA (a), ascribed to a first-stage of coalescence processes, while at 40 mA a more uniform distribution was obtained (b).

In this context it is necessary to recall how the nanoparticles deposition on solid surfaces does not only depend on the sputtering conditions. Nanoparticles with different sizes and shapes can be obtained by sputtering a metal onto different surfaces from the surface chemistry and morphology point of view..[32-34] For this reason the kinetics of metal nanoparticle nucleation on the substrate has a crucial role on the structuration of the as-sputtered material. At the beginning of sputtering deposition of metal onto polymeric surface, a gradient metal diffusion layer within the molecular film can be present at the metal/organic interface.[J. Phys. Chem. Lett., 2013, 4, 3170]. After that adatoms coming from the gas phase are adsorbed onto the solid surface and they can follow three main growth mechanisms.[35] The first one, Frank van der Merwe mode, involves a layer-by-layer growth of mono-adlayers. The second growth is known as Volmer-Weber mode, consist of 3-D adatom clustering on the substrate. The last one, Stranski-Krastanov growth, involves a combination of the previous models resulting in alternated adlayers formation and 3-D clustering.[36]

The most influencing factor of the growth mechanism occurrence is the adatom migration on the surface: after the adatom absorption, they can migrate forming stable nucleus with near neighbors on the surface. ~~If this process does not take place, adatom evaporates back in the gas.~~ Ultra small islands start to appear randomly on the surface and one of the growing modes will be followed in order to minimize their energy.

In our case, the elastomer surface influences the metal film morphology in the initial growth stage: as stated before, the red shift of the plasmonic dip observed in the optical transmittance spectra is directly related to increased Ag NP dimension (and the consequent decrease of the inter-particle gap).

We can suppose that increasing the mixing ratio the evolution of the surface properties (investigated by FTIR analysis) cause a faster diffusion of silver adatom on the PDMS surface. This hypothesis of diffusion difference could be mainly ascribed to the metal-elastomer interaction which strongly depends on the tunable chemistry, stiffness, and surface properties of the PDMS as discussed above (see Figure 1). Actually, we have previously observed that the surface energy of PDMS decreases by increasing the mixing ratio[20] while the Young's modulus behave in opposite direction.[8]

Direct evidences that the adatoms diffusivity influence the growth mode and the nanostructure formation has been published by Ruffino et al.[Appl Phys A, 2011, 103, 939]. In their work the authors evaluate the room temperature surface diffusion coefficient of Au on PS and on PMMA and directly correlate them to the Au work of adhesion on the two different polymers. Their results demonstrate that the Au atom diffusivity is higher on the substrate exhibiting the lower adhesion energy.

Taking into account the above mentioned studies, we evaluated the Ag work of adhesion on PDMS with different mixing ratio. Surface energies of silver and PDMS were calculated exploiting the Wu model [20] starting from the contact angle of both water and diiodomethane. Polar and dispersive components of the surface energies were used to estimate the work of adhesion by a harmonic mean as described in the supporting information. The results (collected in Figure S2) show a monotonic decrease of the adhesion energy by increasing the mixing ratio. Such a behavior does support the above discussed hypothesis. In particular, the increase of the mixing ratio leads to a faster diffusion of silver adatom on the elastomer surface and a consequent enlargement of the Ag nanoparticle sizes, as verified by the red shift of the plasmonic dip observed in the optical transmittance spectra.

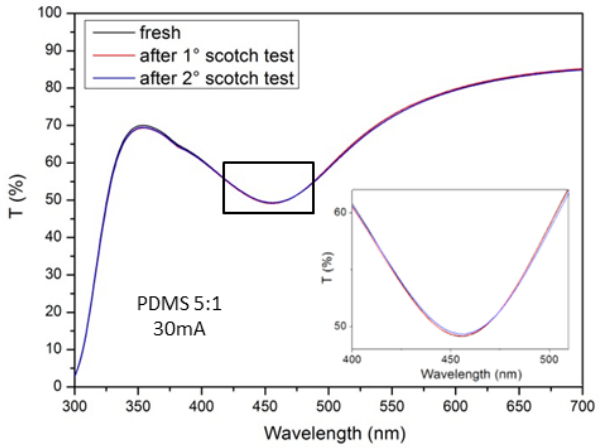

Figure 6. *Transmittance spectra of PDMS membrane coated with Ag nanoparticles by sputtering deposition (mixing ratio 5:1 and deposition current equal to 30 mA) before and after two consecutive scotch tests.*

A simple qualitative test, well known as the 'scotch tape test', was used to examine the adhesion of the Ag nanoparticles to PDMS. Pieces of adhesive tape were firmly placed on the Ag/PDMS surface and a pressure of 22 kPa (about 500 g of weight place onto the sample) was then applied for 1 min. A glass slide was used between the adhesive tapes and the weight in order to apply uniform pressure on the adhesive tapes and PDMS. When the adhesive tapes were released from PDMS, a fraction of the Ag nanoparticles could be transferred to the adhesive tapes depending on the adhesion of the Ag NPs to PDMS.

The optical analysis of the surface (transmittance spectra reported in Figure 6) indicated that there was not removal of the film after the scotch tests evidencing a good adhesion of the sputtered NPs onto PDMS. This finding have enormous importance if the metal-elastomeric nanostructure was used as an active substrate hosting a liquid analytes to be detected by enhanced Raman or fluorescence spectroscopy.[37]

The wettability of the samples was investigated by contact angle (CA) measurements (Figure 7). The measured H_2O CA, related to the bare PDMS samples, slightly increase (average values: 112° → 116°) according to the increase of oligomer/cross-linker ratio as previously reported.[20] This effect is

due to the increasing contribution of the oligomer unreacted fragments for the PDMS high ratio composition (see Figure 1).

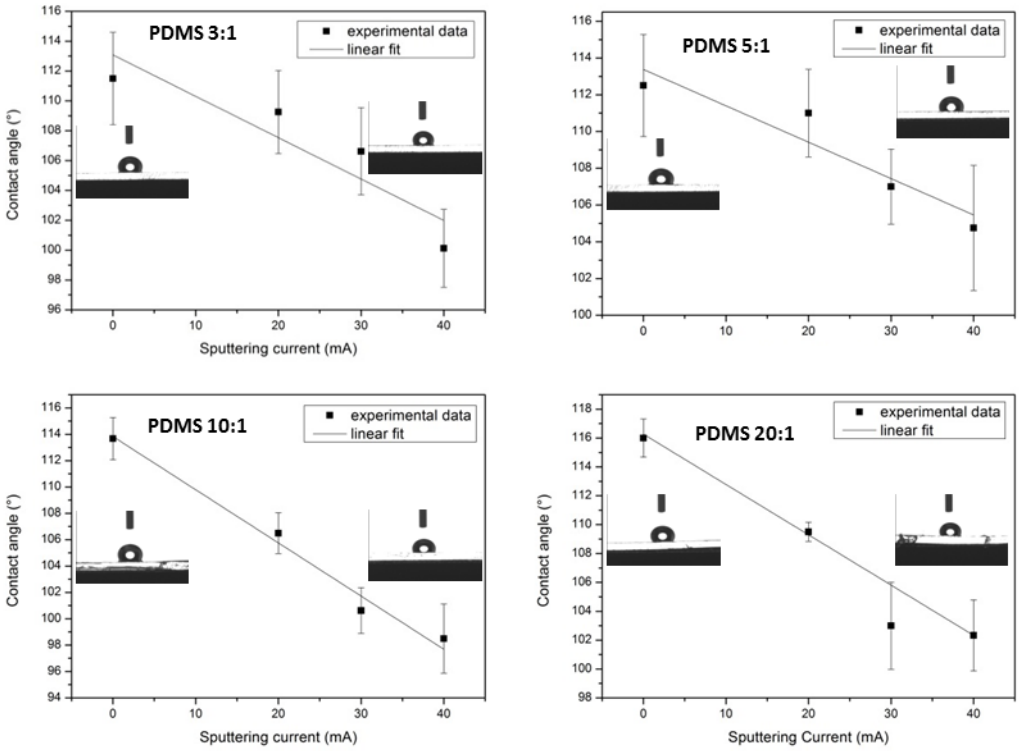

Figure 7. *Water contact angle values of PDMS membrane coated with Ag nanoparticles by sputtering deposition varying the PDMS mixing ratio and the sputtering current at a fixed deposition time of 5 seconds. The insets show, for each PDMS composition, the water drop on PDMS uncoated and coated by 40 mA sputtering current deposition.*

For the silver-coated PDMS samples, according to the increase of sputtering current intensity, the growing coverage of Ag nanoparticles increase the surface hydrophilicity for each studied composition,[2,38] due to progressive decreased contribution of hydrophobic PDMS polymeric chains exposed at the surface.

The wettability of the elastomeric substrates were strongly affected by the sputtering current with a decrease of the H_2O CA of about 10% for each composition with respect to the uncoated samples and a maximum decrease of 13% obtained for the mixing ratio equal to 10:1.

This average CA trend can be directly correlated to the diminishing of the bare PDMS portion exposed to H_2O contact, that is, to the increase of Ag coverage. This amount can be quantified through the filling fraction calculation, i.e. the percentage of sample surface covered by Ag particles, based on the FESEM images (Figure 5a and b): 0.299, 0.435, 0.470 for 20, 30, 40 mA of sputtering current, respectively. The observed hydrophilization effect is supported by the study of Feng and Zhao, through CA analysis and wetting modelling, on a PDMS surface modified by sputtered Au nanostructures.[22]

The high variability (high standard deviation) of measured CA values does not allow an in-depth analysis of the correlation between morphology of growing Ag nanoparticles with respect to the four tested PDMS compositional ratios.

The most reproducible CA were obtained for 10:1 and 20:1 composition at 20mA of sputtering current, where the ratio between the two kind of polymer base components with respect to the Ag coating represent the best compromise in terms of contributions to surface wettability. This suggests that a controllable and reproducible process could be selected.

Finally, the morphology of PDMS surface have been characterized after the deposition of a metal film. Previous study[39] exploiting metal film deposition on elastomer revealed a wavy surface. These complex out-of-plane structures are induced by the heat generated during the deposition and subsequent cooling down of PDMS to room temperature: silicone shrinkage created a compressive stress in the metallic thin film, causing it to buckle out-of-plane.

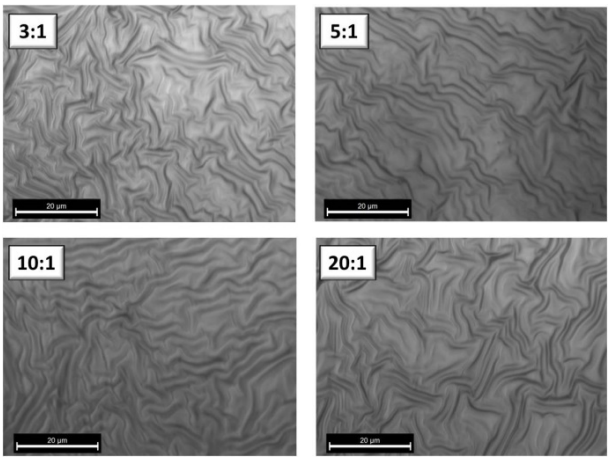

Figure 6. *Optical microscope images (100 X magnification) of 100 nm Pt-coated PDMS surfaces at different mixing ratio (oligomer:crosslinker): 3:1, 5:1, 10:1, 20:1.*

In order to check the effect of PDMS mixing ratio on its surface corrugation a thin Pt film was deposited on the top of PDMS surface to allow an optical characterization. By varying the mixing ratio the morphology did not seem to be dependent on the curing agent concentration: the wrinkles are very similar for all the samples under investigation as shown in Figure 8. Therefore it is possible to exclude the mixing ratio dependence of PDMS surface corrugation on the observed wettability and optical behaviours just related to the elastomeric matrix.

CONCLUSIONS

Herein, the properties of PDMS membranes synthesized with different mixing ratio decorated by Ag nanoparticles via d.c. sputtering was presented and critically discussed. The wettability of the elastomeric substrate was strongly affected by the sputtering current with a decrease of the water contact angle of about 10% for each composition with respect to the uncoated samples. The optical response of the Ag coated PDMS substrates were investigated showing interesting tunable transmittance spectra characterized by plasmonic dips subjected to a spectral red-shift by increasing both the mixing ratio and the sputtering current from 430 nm

up to 510 nm due to the modified Ag nanoparticles morphology, as corroborated by FEM calculations.

Considering the broad spectrum of employ of PDMS, such hybrid substrates can find application in various fields ranging from flexible tunable plasmonic substrates for SERS or metal enhanced fluorescence to microfluidic devices where could be required a tunable wettability.

AUTHOR INFORMATION

Corresponding Author

*E-mail: andrea.lamberti@polito.it. Tel. +39-011-5647394.

Author Contributions

A. L. conceived the idea, fabricated the samples, performed the optical, IR and contact angle characterizations and wrote the paper. A. V. performed FESEM measurements and evaluated the particle size distributions. P. R. discussed the CA measurements. A. A. performed FEM calculations. F. G. conceived the idea, executed the data analysis, and wrote the paper. All authors contributed to the scientific discussion and revision of the article, giving approval to the final version of the manuscript.

Notes

The authors declare no competing financial interest.

ACKNOWLEDGMENTS

This research has received funding from the Italian Flagship Project NANOMAX and the FIRB NEWTON.

REFERENCES

(1) Plecis, A.; Chen, Y., *Microelectron. Eng.* Fabrication of microfluidic devices based on glass–PDMS–glass technology. **2007**, *84*, 1265-1269.

(2) Zhou, J.; Ellis, A. V.; Voelcker, N. H., *Electrophoresis.* Recent developments in PDMS surface modification for microfluidic devices. **2010**, *31*, 2-16.

(3) Lötters, J. C.; Olthuis, W.; Veltink, P. H.; Bergveld, P., *J. Micromech. Microeng.* The mechanical properties of the rubber elastic polymer polydimethylsiloxane for sensor applications. **1997**, *7*, 145.

(4) Sacco, A.; Lamberti, A.; Pugliese, D.; Chiodoni, A.; Shahzad, N.; Bianco, S.; Quaglio, M.; Gazia, R.; Tresso, E.; Pirri, C. F., *Appl. Phys. A – Mater.* Microfluidic housing system: a useful tool for the analysis of dye-sensitized solar cell components. **2012**, *109*, 377-383.

(5) Molberg, M.; Crespy, D.; Rupper, P.; Nüesch, F.; Månson, J. A. E.; Löwe, C.; Opris, D. M. *Adv. Funct. Mater.* High breakdown field dielectric elastomer actuators using encapsulated polyaniline as high dielectric constant filler. **2010**, *20*, 3280-3291.

(6) Zanardi, A.; Bandiera, D.; Bertolini, F.; Corsini, C. A.; Gregato, G.; Milani, P.; Barborini, E.; Carbone, R. *Biotechniques.* Miniaturized FISH for screening of onco-hematological malignancies. **2010**, *49*, 497-504.

(7) Rogers, J. A.; Someya, T.; Huang, Y. *Science.* Materials and mechanics for stretchable electronics. **2010**, *327*, 1603-1607.

(8) Lamberti, A.; Marasso, S.L.; Cocuzza, M. *RSC Advances.* PDMS membranes with tunable gas permeability for microfluidic applications. **2014**, *4*, 61415-61419.

(9) Zuo, P.; Li, X.; Dominguez, D. C.; Ye, B. C. *Lab Chip.* A PDMS/paper/glass hybrid microfluidic biochip integrated with aptamer-functionalized graphene oxide nano-biosensors for one-step multiplexed pathogen detection. **2013**, *13*, 3921-3928.

(10) Descrovi, E.; Frascella, F.; Ballarini, M.; Moi, V.; Lamberti, A.; Michelotti, F.; Giorgis, F.; Pirri, C. F. *Appl. Phys. Lett.* Surface label-free sensing by means of a fluorescent multilayered photonic structure. **2012**, *101*, 131105.

(11) Lee, H. K.; Chung, J.; Chang, S. I.; Yoon, E. *J. Micromech. Microeng.* Real-time measurement of the three-axis contact force distribution using a flexible capacitive polymer tactile sensor. **2011**, *21*, 035010.

(12) Stassi, S.; Canavese, G.; Cosiansi, F.; Gazia, R.; Fallauto, C.; Corbellini, S.; Pirola, M.; Cocuzza, M. *Smart Mater. Struct.* Smart piezoresistive tunnelling composite for flexible robotic sensing skin. **2013**, *22*, 125039.

(13) Bhagat, A. A. S.; Jothimuthu, P.; Papautsky, I. *Lab Chip.* Photodefinable polydimethylsiloxane (PDMS) for rapid lab-on-a-chip prototyping. **2007**, *7*, 1192-1197.

(14) Lamberti, A.; Angelini, A.; Ricciardi, S.; Frascella, F. *Lab Chip.* A flow-through holed PDMS membrane as a reusable microarray spotter for biomedical assays. **2015**, *15*, 67-71.

(15) Fan, F. R.; Lin, L.; Zhu, G.; Wu, W.; Zhang, R.; Wang, Z. L. *Nano Lett.* Transparent triboelectric nanogenerators and self-powered pressure sensors based on micropatterned plastic films. **2012**, *12*, 3109-3114.

(16) Bella, F.; Lamberti, A.; Sacco, A.; Bianco, S.; Chiodoni, A.; Bongiovanni, R. *J. Membrane Sci.* Novel electrode and electrolyte membranes: Towards flexible dye-sensitized solar cell combining vertically aligned TiO_2 nanotube array and light-cured polymer network. **2014**, *470*, 125-131.

(17) Maleki, T.; Chitnis, G.; Ziaie, B. *J. Micromech. Microeng.* A batch-fabricated laser-micromachined PDMS actuator with stamped carbon grease electrodes. **2011**, *21*, 027002.

(18) Lamberti, A.; Di Donato, M.; Chiappone, A.; Giorgis, F.; Canavese, G. *Smart Mater. Struct.* Tunable electromechanical actuation in silicone dielectric film. **2014**, *23*, 105001.

(19) Carrillo, F.; Gupta, S.; Balooch, M.; Marshall, S. J.; Marshall, G. W.; Pruitt, L.; Puttlitz, C. M. *J. Mater. Res.* Nanoindentation of polydimethylsiloxane elastomers: Effect of

crosslinking, work of adhesion, and fluid environment on elastic modulus. **2005**, *20*, 2820-2830.

(20) Lamberti, A.; Quaglio, M.; Sacco, A.; Cocuzza, M.; Pirri, C. F. *Appl. Surf. Sci.* Surface energy tailoring of glass by contact printed PDMS. **2012**, *258*, 9427-9431.

(21) Kommireddy, D. S.; Patel, A. A.; Shutava, T. G.; Mills, D. K.; Lvov, Y. M. *J. Nanosci. Nanotechnol.* Layer-by-layer assembly of TiO2 nanoparticles for stable hydrophilic biocompatible coatings. **2005**, *5*, 1081-1087.

(22) Lamberti, A.; Microfluidic photocatalytic device exploiting PDMS/TiO_2 nanocomposite, Appl. Surf. Sci. **2015,** in press, http://dx.doi.org/10.1016/j.apsusc.2015.01.239.

(23) Kim, K. S.; Zhao, Y.; Jang, H.; Lee, S. Y.; Kim, J. M.; Kim, K. S.; Ahn, J-H.; Kim, P.; Choi, J-Y.; Hong, B. H. *Nature.* Large-scale pattern growth of graphene films for stretchable transparent electrodes. **2009**, *457*, 706-710.

(24) Fang, C.; Shao, L.; Zhao, Y.; Wang, J.; Wu, H. *Adv. Mater.* A gold nanocrystal/poly (dimethylsiloxane) composite for plasmonic heating on microfluidic chips. **2012**, *24*, 94-98.

(25) Huang, F.; Baumberg, J. J. *Nano Lett.* Actively tuned plasmons on elastomerically driven Au nanoparticle dimers. **2010**, *10*, 1787-1792.

(26) Hossain, M. K.; Willmott, G. R.; Etchegoin, P. G.; Blaikie, R. J.; Tallon, J. L. *Nanoscale*. Tunable SERS using gold nanoaggregates on an elastomeric substrate. **2013**, *5*, 8945-8950.

(27) Lamberti, A.; Virga, A.; Angelini, A.; Ricci, A.; Descrovi, E.; Cocuzza, M.; Giorgis, F. *RSC Advances*. Metal–elastomer nanostructures for tunable SERS and easy microfluidic integration. **2015**, *5*, 4404-4410.

(28) Mertens, H.; Verhoeven, J.; Polman, A.; Tichelaar, F. D. *Appl. Phys. Lett.* Infrared surface plasmons in two-dimensional silver nanoparticle arrays in silicon. **2004**, *85*, 1317-1319.

(29) Virga, A.; Gazia, R.; Pallavidino, L.; Mandracci, P.; Descrovi, E.; Chiodoni, A.; Geobaldo, F.; Giorgis, F. *Phys. Status Solidi C.* Metal-dielectric nanostructures for amplified Raman and fluorescence spectroscopy. **2010**, *7*, 1196-1199.

(30) Novara, C.; Petracca, F.; Virga, A.; Rivolo, P.; Ferrero, S.; Geobaldo, F.; Porro, S.; Giorgis, F. *Nanoscale Res. Lett.* SERS active silver nanoparticles synthesized by inkjet printing on mesoporous silicon. **2014**, *9*, 1-7.

(31) Ramalingam, B.; Mukherjee, S.; Mathai, C. J.; Gangopadhyay, K.; Gangopadhyay, S. *Nanotechnology*. Sub-2 nm size and density tunable platinum nanoparticles using room temperature tilted-target sputtering **2013**, *24*, 205602.

(32) Kaune, G.; Metwalli, E.; Meier, R.; Körstgens, V.; Schlage, K.; Couet, S.; Röhlsberger, R.; Roth, S. V.; Müller-Buschbaum, P. *ACS Appl. Mater. Interfaces*. Growth and morphology of sputtered aluminum thin films on P3HT surfaces. **2011**, *3*, 1055-1062.

(33) Chaloupka, A.; Šimek, P.; Šutta, P.; Švorčík, V. *Mater. Lett.* Influence of substrate on properties of gold nanolayers. **2010**, *64*, 1316-1318.

(34) Kaune, G.; Ruderer, M. A.; Metwalli, E.; Wang, W.; Couet, S.; Schlage, K.; Röhlsberger, R.; Roth, S. V.; Muller-Buschbaum, P. *ACS Appl. Mater. Interfaces*. In situ GISAXS study of gold film growth on conducting polymer films. **2008**, *1*, 353-360.

(35) Koch, R. *Surf. Coat. Technol.* Stress in evaporated and sputtered thin films–a comparison. **2010**, *204*, 1973-1982.

(36) Bauer, E.; van der Merwe, J. H. *Phys. Rev. B.* Structure and growth of crystalline superlattices: From monolayer to superlattice. **1986**, *33*, 3657.

(37) Parisi, J.; Su L.; Lei, Y. *Lab Chip*. In situ synthesis of silver nanoparticle decorated vertical nanowalls in a microfluidic device for ultrasensitive in-channel SERS sensing. **2013**, *13*, 1501-1508.

(38) Feng, J-T.; Zhao, Y-P. *Biomed. Microdev.* Influence of different amount of Au on the wetting behavior of PDMS membrane. **2008**, *10*, 65-72.

(39) Bowden, N.; Huck, W. T.; Paul, K. E.; Whitesides, G. M. *Appl. Phys. Lett.* The controlled formation of ordered, sinusoidal structures by plasma oxidation of an elastomeric polymer. **1999**, 75, 2557-2559.